

Steady symmetrical temperature field in a hollow spherical particle with temperature-dependent thermal conductivity

A. MOOSAIE

*Department of Mechanical Engineering
Yasouj University
75914-353 Yasouj, Iran
e-mail: aminmoosaie@gmail.com*

IN THIS WORK, AN EXACT ANALYTICAL SOLUTION to the axisymmetric heat conduction equation for hollow spherical objects with temperature-dependent thermal conductivity is presented. The nonlinear differential equation is first transformed into a linear one by means of an integral transform method. Then, the separation of variables method is employed to solve the transformed linear equation. Ultimately, we use the inverse transform to obtain the physical temperature field. Furthermore, two examples are worked out, i.e., the one-dimensional heat conduction in the radial direction and the two-dimensional case with axial symmetry. The solution is presented as an infinite series in terms of Legendre functions. The problem with spherical symmetry is also solved by using perturbation methods up to the third-order approximation, and the results are compared with the exact solution.

Key words: heat conduction, steady-state, analytical solution, temperature-dependent thermal conductivity, nonlinear equation, hollow sphere.

Copyright © 2012 by IPPT PAN

1. Introduction

HEAT CONDUCTION IN SPHERICAL OBJECTS is an important problem in engineering practice. It is also an interesting problem from a fundamental/mathematical point of view. Analytical methods are often limited to linear problems, i.e., problems with linear differential equations and boundary conditions. In heat conduction context, this implies a constant or at most a space-dependent (but not temperature-dependent) thermal conductivity. However, the assumption of a constant thermal conductivity is valid when the range of temperatures involved is not wide. When we encounter a wide range of temperatures in a problem, then the temperature dependence of the thermal conductivity is usually to be taken into account.

Analytical solution of linear heat conduction problem in a spherical object is a rather classical problem, see for example [1]. Also, some recent analytical works can be found on the non-Fourier heat conduction in a hollow sphere [2, 3]. However, these are linear cases. Analytical solutions for nonlinear cases

with temperature-dependent thermal conductivity are rare. Trostel [4, 5] has proposed a method to treat this kind of problems analytically using the Kirchhoff's transform. He has applied his method to the one-dimensional problem of nonlinear heat conduction in a hollow cylinder (in the radial direction). A perturbation method is utilized in [6] to solve the nonlinear heat conduction problem in a fin with temperature-dependent thermal conductivity. The homotopy analysis method (HAM) is used in [7] to analytically investigate the thermal performance of a straight fin of trapezoidal profile with temperature-dependent thermal conductivity. Hybrid analytical-numerical methods are becoming more attractive among researchers. Often in these approaches, the nonlinear governing equation is reduced in dimensions by using some symmetry arguments, e.g., by using the Lie group theory, and then the reduced problem (usually an ordinary differential equation) is solved numerically, e.g., see [8].

In this work, we analytically solve the problems of spherically-symmetric and axisymmetric heat conduction in a hollow sphere with temperature-dependent thermal conductivity. The solution to this nonlinear problem is obtained as an infinite series in terms of Legendre functions. We make use of the Kirchhoff's integral transform to solve the problem.

The remainder of this paper is organized as follows. The governing differential equations are presented in Sec. 2. Section 3 contains the solution method in general and the application of the general solution to hollow spherical objects with worked-out examples. The paper is concluded in Sec. 4.

2. Governing equations

In this section, we present the governing equations of steady heat conduction in a hollow sphere with temperature-dependent thermal conductivity. For this purpose, we start with the steady energy conservation equation without heat generation:

$$(2.1) \quad \nabla \cdot \mathbf{q} = 0,$$

where ∇ and \mathbf{q} are the nabla operator and heat flux vector, respectively. This is a scalar equation

$$(2.2) \quad \frac{\partial q_i}{\partial x_i} = \frac{\partial q_1}{\partial x_1} + \frac{\partial q_2}{\partial x_2} + \frac{\partial q_3}{\partial x_3} = 0,$$

for three components of the heat flux vector \mathbf{q} , i.e., q_i 's. In order to close the system, we require a constitutive equation. In this work, we use the Fourier heat conduction law:

$$(2.3) \quad \mathbf{q} = -\lambda \cdot \nabla \vartheta,$$

in which the scalar quantity ϑ is the temperature, and $\boldsymbol{\lambda}$ is the thermal conductivity tensor. For isotropic materials, the thermal conductivity tensor $\boldsymbol{\lambda}$ reduces to a spherical tensor, i.e.,

$$(2.4) \quad \boldsymbol{\lambda} = \lambda \mathbf{1},$$

with λ and $\mathbf{1}$ being the thermal conductivity and the identity tensor, respectively. Substituting Eq. (2.4) into Eq. (2.3) yields

$$(2.5) \quad \mathbf{q} = -\lambda \nabla \vartheta.$$

The Fourier constitutive equation (2.5) along with the energy conservation equation (2.1) gives the following field equation for the temperature:

$$(2.6) \quad \nabla \cdot (\lambda \nabla \vartheta) = \nabla \lambda \cdot \nabla \vartheta + \lambda \Delta \vartheta = 0,$$

where Δ is the Laplacian operator. The thermal conductivity λ can depend on the spatial coordinates (e.g., due to material inhomogeneities) and/or temperature. The former case leads to a linear partial differential equation (PDE) with variable coefficients whereas the latter case results in a nonlinear PDE. In the simplest case, λ is assumed to be a constant (with $\nabla \lambda = \mathbf{0}$), and Eq. (2.6) reduces to the Laplace equation:

$$(2.7) \quad \Delta \vartheta = 0.$$

Experimental observations show that, in general, λ does depend on temperature, i.e., $\lambda = \lambda(\vartheta)$ [9]. The assumption of a constant thermal conductivity is a good approximation when the range of temperatures involved is small. This assumption is often made because it offers a great simplification in the mathematical analysis of heat conduction problems. However, in problems which involve a broad range of temperatures, this assumption becomes less accurate and one needs to take into account the dependence of λ on the temperature. By doing so, we have

$$\nabla \lambda = \frac{d\lambda}{d\vartheta} \nabla \vartheta,$$

and Eq. (2.6) reads

$$(2.8) \quad \frac{d\lambda}{d\vartheta} \nabla \vartheta \cdot \nabla \vartheta + \lambda(\vartheta) \Delta \vartheta = 0,$$

which is obviously nonlinear.

In the next section, we analytically solve the nonlinear problem of heat conduction in hollow spherical objects with temperature-dependent thermal conductivity.

3. Analytical solution

In this section, we present analytical solutions to the nonlinear PDE (2.6) (or (2.8)) in hollow spherical objects with inner and outer radii r_i and r_o , respectively. First, we present the solution strategy for this type of problems in Subsec. 3.1. Then, we proceed to solve the nonlinear PDE (2.6) in the spherical coordinate system shown in Fig. 1. In general, for a steady three-dimensional case we have $\vartheta = \vartheta(r, \psi, \varphi)$. However, we consider two reduced cases in this paper. The first case, presented in Subsec. 3.2, considers the temperature field with spherical symmetry (one-dimensional in the radial direction), that is

$$(3.1) \quad \frac{\partial \vartheta}{\partial \psi} = \frac{\partial \vartheta}{\partial \varphi} = 0, \quad \vartheta = \vartheta(r).$$

The second case, presented in Subsec. 3.3, is the axisymmetric case (two-dimensional) which takes place when

$$(3.2) \quad \frac{\partial \vartheta}{\partial \varphi} = 0, \quad \vartheta = \vartheta(r, \psi).$$

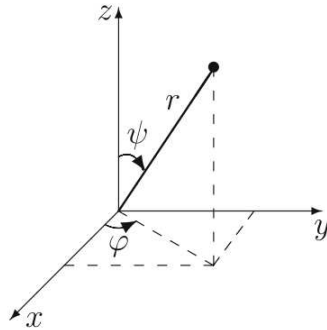


FIG. 1. Spherical coordinate system.

3.1. Solution strategy

Trostel [4] has developed a methodology to deal with the nonlinear equation (2.6). It is based on the following integral transform of the temperature field:

$$(3.3) \quad \Theta(\vartheta) = \frac{1}{\lambda_0} \int_{\tilde{\vartheta}=0}^{\vartheta} \lambda(\tilde{\vartheta}) d\tilde{\vartheta}, \quad \lambda_0 = \lambda(\vartheta = 0).$$

Taking the gradient of Eq. (3.3) we have

$$(3.4) \quad \nabla \Theta = \frac{1}{\lambda_0} \lambda(\vartheta) \nabla \vartheta,$$

in which the Leibniz integral theorem is used. Substitution of Eq. (3.4) into the nonlinear heat equation (2.6) yields the Laplace partial differential equation for the transformed temperature Θ :

$$(3.5) \quad \Delta\Theta = 0.$$

It is seen that we obtain a linear PDE which can be solved analytically. The nonlinearity now lies in the integral transform (3.3), that is, Θ nonlinearly depends on ϑ and vice versa.

For a wide range of engineering materials, one can assume a linear dependence of the thermal conductivity λ on the temperature ϑ , that is

$$(3.6) \quad \lambda(\vartheta) = \lambda_0 - \lambda_1\vartheta,$$

with λ_0 and λ_1 being material constants. Inserting Eq. (3.6) into the integral transform (3.3) results in

$$(3.7) \quad \Theta(\vartheta) = \vartheta - \frac{\varepsilon}{2}\vartheta^2, \quad \varepsilon = \frac{\lambda_1}{\lambda_0}.$$

The nonlinear algebraic equation (3.7) describes the transformed temperature Θ as a function of the physical temperature ϑ . In turn, one can derive an equation for ϑ in terms of Θ by inverting (3.7):

$$(3.8) \quad \vartheta_{1,2}(\Theta) = \frac{1}{\varepsilon} \left(1 \pm \sqrt{1 - 2\varepsilon\Theta} \right).$$

In order to decide which sign reveals physically acceptable temperatures, we look at the integral transform (3.3) in the limiting case $\lambda_1 \rightarrow 0$ (i.e., $\varepsilon \rightarrow 0$) which represents the case of a constant thermal conductivity. Equations (3.3) and (3.7) show that $\vartheta = \Theta$ in this case. Now, we take the limit of expression (3.9) as $\varepsilon \rightarrow 0$. For the plus sign, we have

$$\lim_{\varepsilon \rightarrow 0} \vartheta_1 = \lim_{\varepsilon \rightarrow 0} \frac{1}{\varepsilon} \left(1 + \sqrt{1 - 2\varepsilon\Theta} \right) = \frac{2}{0} = \infty.$$

For the minus sign, one writes

$$\lim_{\varepsilon \rightarrow 0} \vartheta_2 = \lim_{\varepsilon \rightarrow 0} \frac{1}{\varepsilon} \left(1 - \sqrt{1 - 2\varepsilon\Theta} \right) = \frac{0}{0}.$$

Using the l'Hopital's rule, we have

$$\lim_{\varepsilon \rightarrow 0} \vartheta_2 = \lim_{\varepsilon \rightarrow 0} \frac{1 - \sqrt{1 - 2\varepsilon\Theta}}{\varepsilon} = \lim_{\varepsilon \rightarrow 0} \left(-\frac{1}{2} \right) (-2\Theta) \frac{1}{\sqrt{1 - 2\varepsilon\Theta}} = \Theta.$$

Therefore, we choose the minus sign which yields

$$(3.9) \quad \vartheta(\Theta) = \frac{1}{\varepsilon} \left(1 - \sqrt{1 - 2\varepsilon\Theta} \right).$$

It shall be noted here that Eq. (3.9) yields physical temperatures when $2\varepsilon\Theta < 1$ or $\Theta < 1/2\varepsilon$. This might seem too restrictive at the first glance. However, such inequality typically holds for engineering materials over a considerable range of temperatures. For example, for mild steel we have $\varepsilon = 5.83 \times 10^{-4}$ and thus $\Theta < 857$ which translates to $\vartheta < 1714^\circ\text{C}$.

3.2. Case with spherical symmetry

In this case, the temperature only depends on the radial coordinate and we have $\vartheta = \vartheta(r)$. Thus, the governing Eq. (2.6) reduces to

$$(3.10) \quad \nabla \cdot [\lambda(\vartheta) \nabla \vartheta] = \frac{1}{r^2} \frac{d}{dr} \left[r^2 \lambda(\vartheta) \frac{d\vartheta}{dr} \right] = 0.$$

The Dirichlet's boundary conditions are

$$(3.11) \quad \vartheta(r = r_i) = \vartheta_i, \quad \vartheta(r = r_o) = \vartheta_o.$$

Using the linear dependence of λ on temperature (3.6) and the transform (3.7), the governing Eq. (3.10) in terms of the transformed temperature Θ reads

$$(3.12) \quad \Delta\Theta = \frac{1}{r^2} \frac{d}{dr} \left(r^2 \frac{d\Theta}{dr} \right) = 0.$$

This is a Cauchy–Euler differential equation with the general solution:

$$(3.13) \quad \Theta(r) = C_1 + \frac{C_2}{r}.$$

The integration constants C_1 and C_2 are to be determined from the boundary conditions. To this aim, we first need to transform the boundary conditions (3.11):

$$(3.14) \quad \begin{aligned} \Theta(r = r_i) &= \vartheta_i - \frac{\varepsilon}{2} \vartheta_i^2 = \Theta_i, \\ \Theta(r = r_o) &= \vartheta_o - \frac{\varepsilon}{2} \vartheta_o^2 = \Theta_o. \end{aligned}$$

Applying Eq. (3.14) to Eq. (3.13) we have

$$(3.15) \quad \begin{aligned} C_1 &= \Theta_i - \frac{r_o}{r_i - r_o} (\Theta_o - \Theta_i) = \frac{r_o \Theta_o - r_i \Theta_i}{r_o - r_i}, \\ C_2 &= \frac{r_i r_o}{r_i - r_o} (\Theta_o - \Theta_i). \end{aligned}$$

As an example, here we consider a hollow sphere with $r_i = 0.6$ cm and $r_o = 1.0$ cm. The boundary temperatures are assumed to be $\vartheta_i = 0.0^\circ\text{C}$ and $\vartheta_o = 1000.0^\circ\text{C}$. Three cases are considered. First, we consider a constant thermal conductivity which leads to the linear differential equation (2.7) for the temperature field. In this case, the temperature field is independent of the value of the thermal conductivity. As for the second case, we consider a sphere made of mild steel for which we have [4]

$$\lambda_0 = 0.12 \text{ cal cm}^{-1} \text{ sec}^{-1} \text{ }^\circ\text{C}^{-1}, \quad \lambda_1 = 7 \times 10^{-5} \text{ cal cm}^{-1} \text{ sec}^{-1} \text{ }^\circ\text{C}^{-2}.$$

A positive λ_1 means that the thermal conductivity decreases with increasing the temperature. Also, we present another fictitious material with

$$\lambda_0 = 0.12 \text{ cal cm}^{-1} \text{ sec}^{-1} \text{ }^\circ\text{C}^{-1}, \quad \lambda_1 = -7 \times 10^{-5} \text{ cal cm}^{-1} \text{ sec}^{-1} \text{ }^\circ\text{C}^{-2},$$

whose thermal conductivity increases with increasing the temperature. The temperature profiles for the above-mentioned cases are shown in Fig. 2. For the first case with constant λ we have $\vartheta = \Theta$ and we get the classical solution. For the second case (mild steel) the temperature profile deviates from the first case. Except from the boundaries r_i and r_o , the temperature is lower across the sphere thickness. $\partial\vartheta/\partial r$ of the nonlinear temperature is smaller than that of the linear one in the vicinity of the inner surface and gets larger by approaching the outer surface. For the third case with $\lambda_1 = -7 \times 10^{-5}$, we have the opposite behavior. The temperature is greater across the sphere thickness. The temperature gradient is greater than that of the linear temperature adjacent to the inner surface and it gets smaller by approaching the outer surface.

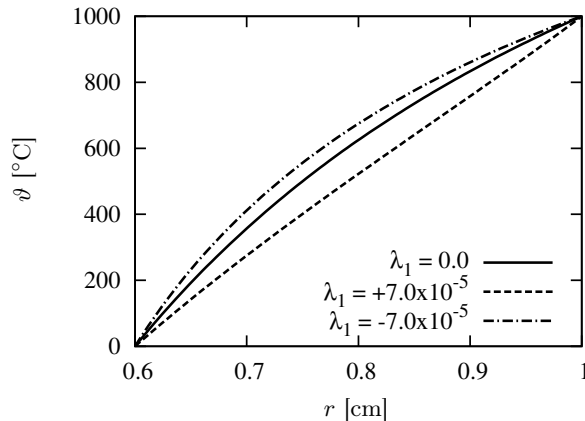


FIG. 2. Spherically symmetric temperature profiles in a hollow sphere with $r_i = 0.6$ cm, $r_o = 1.0$ cm, $\vartheta_i = 0^\circ\text{C}$, $\vartheta_o = 1000^\circ\text{C}$ and $\lambda = \lambda_0 - \lambda_1\vartheta$ with $\lambda_0 = 0.12$. Three cases are shown: constant λ , λ decreasing with temperature and λ increasing with temperature. Values of λ_1 are shown in the figure.

It should be noted here that the nonlinear effects are pronounced when the temperature range is wide. For example, if we reduce ϑ_o from 1000°C to 400°C , we observe that the two temperature profiles with non-zero λ_1 approach the one with zero λ_1 , as shown in Fig. 3. If we decrease the temperature difference even more, say $\vartheta_o = 1^\circ\text{C}$, then the three profiles fall on top of each other, see Fig. 4. This shows that for applications involving a wide range of temperatures, one has to take the nonlinearity into account. However, when the temperature range is narrow, the linear model with constant λ is sufficiently accurate.

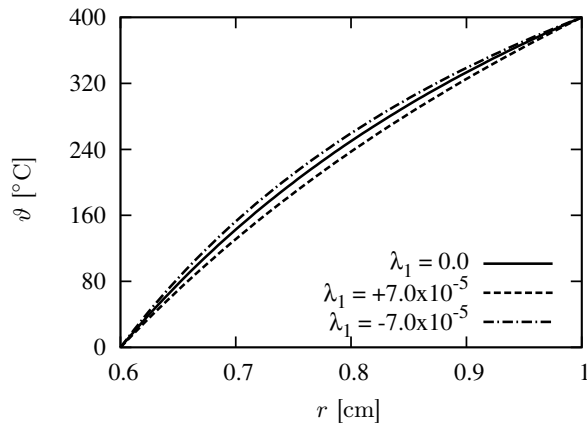


FIG. 3. Spherically symmetric temperature profiles in a hollow sphere with $r_i = 0.6$ cm, $r_o = 1.0$ cm, $\vartheta_i = 0^\circ\text{C}$, $\vartheta_o = 400^\circ\text{C}$ and $\lambda = \lambda_0 - \lambda_1\vartheta$ with $\lambda_0 = 0.12$. Three cases are shown: constant λ , λ decreasing with temperature and λ increasing with temperature. Values of λ_1 are shown in the figure.

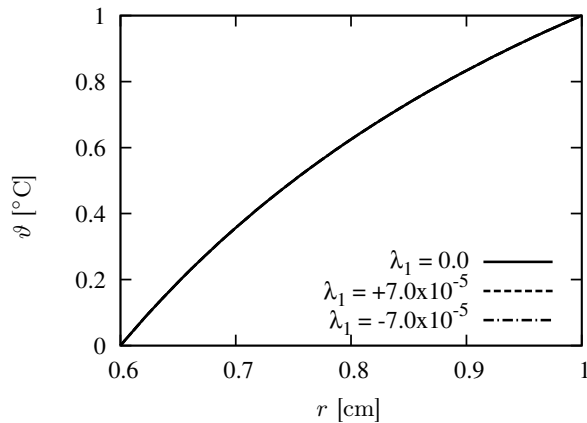


FIG. 4. Spherically symmetric temperature profiles in a hollow sphere with $r_i = 0.6$ cm, $r_o = 1.0$ cm, $\vartheta_i = 0^\circ\text{C}$, $\vartheta_o = 1^\circ\text{C}$ and $\lambda = \lambda_0 - \lambda_1\vartheta$ with $\lambda_0 = 0.12$. Three cases are shown: constant λ , λ decreasing with temperature and λ increasing with temperature. Values of λ_1 are shown in the figure. All three cases lie on top of each other.

3.3. Case with axial symmetry

For the axisymmetric case with $\lambda = \lambda_0 - \lambda_1\vartheta$, the governing Eq. (2.8) reduces to the following nonlinear PDE:

$$(3.16) \quad -\lambda_1 \left[\left(\frac{\partial\vartheta}{\partial r} \right)^2 + \frac{1}{r^2} \left(\frac{\partial\vartheta}{\partial\psi} \right)^2 \right] + (\lambda_0 - \lambda_1\vartheta) \left[\frac{\partial^2\vartheta}{\partial r^2} + \frac{2}{r} \frac{\partial\vartheta}{\partial r} + \frac{1}{r^2} \left(\frac{\partial^2\vartheta}{\partial\psi^2} + \cot\psi \frac{\partial\vartheta}{\partial\psi} \right) \right] = 0.$$

The Dirichlet’s boundary conditions read

$$(3.17) \quad \vartheta(r = r_i, \psi) = \vartheta_i(\psi), \quad \vartheta(r = r_o, \psi) = \vartheta_o(\psi).$$

Using the temperature transform (3.7), Eq. (3.16) reduces to the Laplace equation for the transformed temperature Θ :

$$(3.18) \quad \Delta\Theta = \frac{\partial^2\Theta}{\partial r^2} + \frac{2}{r} \frac{\partial\Theta}{\partial r} + \frac{1}{r^2} \left(\frac{\partial^2\Theta}{\partial\psi^2} + \cot\psi \frac{\partial\Theta}{\partial\psi} \right),$$

subjected to the transformed boundary conditions

$$(3.19a) \quad \Theta(r = r_i, \psi) = \vartheta_i(\psi) - \frac{\varepsilon}{2} (\vartheta_i(\psi))^2 = \Theta_i(\psi),$$

$$(3.19b) \quad \Theta(r = r_o, \psi) = \vartheta_o(\psi) - \frac{\varepsilon}{2} (\vartheta_o(\psi))^2 = \Theta_o(\psi).$$

Now, we solve this problem by the use of a separation ansatz as $\Theta(r, \psi) = R(r)\Psi(\psi)$. Substituting this ansatz into Eq. (3.18) yields

$$(3.20) \quad r^2 \frac{d^2 R_n}{dr^2} + 2r \frac{dR_n}{dr} - n(n+1) R_n(r) = 0,$$

$$(3.21) \quad \frac{d^2 \Psi_n}{d\psi^2} + \cot\psi \frac{d\Psi_n}{d\psi} + n(n+1) \Psi_n(\psi) = 0.$$

Equation (3.20) is the Cauchy–Euler differential equation and its general solution reads

$$(3.22) \quad R_n(r) = A_{1n} r^n + \frac{B_{1n}}{r^{n+1}}.$$

Equation (3.21) can be rewritten as

$$\frac{1}{\sin\psi} \frac{d}{d\psi} \left(\sin\psi \frac{d\Psi_n}{d\psi} \right) + n(n+1) \Psi_n(\psi) = 0.$$

We now utilize the following transform of angle ψ :

$$(3.23) \quad \Psi_n(\psi) = \Psi_n(\xi(\psi))$$

with $\xi(\psi) = \cos \psi$, $1 - \xi^2 = \sin^2 \psi$ and $\frac{d\xi}{d\psi} = -\sin \psi$.

Applying this transform to Eq. (3.21), we obtain the Legendre differential equation in terms of ξ :

$$(3.24) \quad \frac{d}{d\xi} \left[(1 - \xi^2) \frac{d\Psi_n}{d\xi} \right] + n(n+1) \Psi_n(\xi) = 0,$$

which has the following general solution.

$$(3.25) \quad \Psi_n(\xi) = \Psi_n(\cos \psi) = A_{2n} P_n(\xi) + B_{2n} Q_n(\xi),$$

where $P_n(\xi)$ and $Q_n(\xi)$ are the spherical functions, i.e., Legendre functions, of first and second kind, respectively. Since we have $|\xi| = |\cos \psi| \leq 1$ and the spherical function of second kind is not defined on this interval, the general solution (3.25) reduces to

$$(3.26) \quad \Psi_n(\xi) = \Psi_n(\cos \psi) = A_{2n} P_n(\xi).$$

With the help of abbreviations $A_n = A_{1n} A_{2n}$ and $B_n = B_{1n} A_{2n}$ we have

$$R_n(r) \Psi_n(\psi) = \left(A_n r^n + \frac{B_n}{r^{n+1}} \right) P_n(\xi).$$

Therefore, the transformed temperature field becomes

$$(3.27) \quad \Theta(r, \cos \psi) = \Theta(r, \xi) = \sum_{n=0}^{\infty} R_n(r) \Psi_n(\psi)$$

$$= \sum_{n=0}^{\infty} \left(A_n r^n + \frac{B_n}{r^{n+1}} \right) P_n(\xi).$$

Now, we have to determine the coefficients A_n and B_n ($n = 0, 1, 2, \dots$) by enforcing the boundary conditions (3.19). The transformed boundary temperatures are functions of ψ whereas the transformed temperature field is a function of ψ through $\xi = \cos \psi$. Therefore, we write the functions $\Theta_o(\psi)$ and $\Theta_i(\psi)$ as $\Theta_o = \Theta_o(\xi) = \Theta_o(\cos \psi)$ and $\Theta_i = \Theta_i(\xi) = \Theta_i(\cos \psi)$. By doing so, we have

$$(3.28) \quad \begin{cases} A_n r_o^n + B_n r_o^{-(n+1)} = c_n^{(o)}, \\ A_n r_i^n + B_n r_i^{-(n+1)} = c_n^{(i)}, \end{cases}$$

in which the functions $\Theta_o(\xi)$ and $\Theta_i(\xi)$ are expanded as

$$(3.29a) \quad \Theta_o(\xi) = \sum_{n=0}^{\infty} c_n^{(o)} P_n(\xi),$$

$$(3.29b) \quad \Theta_i(\xi) = \sum_{n=0}^{\infty} c_n^{(i)} P_n(\xi).$$

The coefficients $c_n^{(o)}$ and $c_n^{(i)}$ are determined from the orthogonality of spherical functions $P_n(\xi)$ on the interval $\xi \in [-1, +1]$, namely

$$(3.30) \quad \int_{-1}^{+1} P_n(\xi) P_m(\xi) d\xi = \begin{cases} 0, & m \neq n, \\ \frac{2}{2n+1}, & m = n. \end{cases}$$

This yields

$$(3.31a) \quad c_n^{(o)} = \frac{2n+1}{2} \int_{-1}^{+1} \Theta_o(\xi) P_n(\xi) d\xi,$$

$$(3.31b) \quad c_n^{(i)} = \frac{2n+1}{2} \int_{-1}^{+1} \Theta_i(\xi) P_n(\xi) d\xi.$$

Now, the constants A_n and B_n ($n = 0, 1, 2, \dots$) are obtained by solving the linear equation system (3.28):

$$(3.32a) \quad A_n = \alpha_n^{(i)} c_n^{(i)} + \alpha_n^{(o)} c_n^{(o)},$$

$$(3.32b) \quad B_n = \beta_n^{(i)} c_n^{(i)} + \beta_n^{(o)} c_n^{(o)},$$

where

$$(3.33a) \quad \alpha_n^{(o)} = \frac{r_i^{-(n+1)}}{\Delta_n},$$

$$(3.33b) \quad \alpha_n^{(i)} = -\frac{r_o^{-(n+1)}}{\Delta_n},$$

$$(3.33c) \quad \beta_n^{(o)} = -\frac{r_i^n}{\Delta_n},$$

$$(3.33d) \quad \beta_n^{(i)} = \frac{r_o^n}{\Delta_n},$$

in which

$$(3.33e) \quad \Delta_n = r_o^n r_i^{-(n+1)} - r_o^{-(n+1)} r_i^n.$$

Thus, the transformed temperature field Θ can be written as

$$(3.34) \quad \Theta(r, \xi) = \sum_{n=0}^{\infty} \eta_n(r) P_n(\xi),$$

where

$$(3.35) \quad \eta_n(r) = (\alpha_n^{(i)} c_n^{(i)} + \alpha_n^{(o)} c_n^{(o)}) r^n + (\beta_n^{(i)} c_n^{(i)} + \beta_n^{(o)} c_n^{(o)}) r^{-(n+1)}.$$

Finally, the temperature field $\vartheta(r, \psi) = \vartheta(r, \xi)$ can be obtained by utilizing the inverse transform (3.9):

$$(3.36) \quad \begin{aligned} \vartheta(r, \xi) &= \frac{1}{\varepsilon} \left(1 - \sqrt{1 - 2\varepsilon\Theta(r, \xi)} \right) \\ &= \frac{1}{\varepsilon} \left[1 - \left(1 - 2\varepsilon \sum_{n=0}^{\infty} \eta_n(r) P_n(\xi) \right)^{1/2} \right]. \end{aligned}$$

First, we show that for $\vartheta_i(\psi) = \vartheta_i$ and $\vartheta_o(\psi) = \vartheta_o$, the solution (3.34) reduces to the one-dimensional solution (3.13) with integration constants given by (3.15). For this purpose, we start with constants (3.31):

$$(3.37a) \quad c_n^{(o)} = \Theta_o \int_{-1}^{+1} P_n(\xi) d\xi = \begin{cases} \Theta_o, & n = 0, \\ 0, & n \geq 1. \end{cases}$$

$$(3.37b) \quad c_n^{(i)} = \Theta_i \int_{-1}^{+1} P_n(\xi) d\xi = \begin{cases} \Theta_i, & n = 0, \\ 0, & n \geq 1. \end{cases}$$

This means that only the term with $n = 0$ is non-zero in the series (3.34) and all other terms with $n \geq 1$ vanish. From Eq. (3.33e) we have $\Delta_0 = (r_o - r_i)/r_i r_o$. The solution (3.34) reduces to

$$(3.38) \quad \Theta(r) = A_0 + \frac{B_0}{r},$$

with

$$(3.39a) \quad A_0 = \frac{r_o \Theta_o - r_i \Theta_i}{r_o - r_i},$$

$$(3.39b) \quad B_0 = \frac{r_i r_o}{r_i - r_o} (\Theta_o - \Theta_i).$$

This is exactly the solution we obtained in Subsec. 3.2.

As an example here, we solve the case with $\vartheta_i(\psi) = 0^\circ\text{C}$ and $\vartheta_o(\psi) = \vartheta_o \sin \psi$ with $\vartheta_o = 1000^\circ\text{C}$. Again, we have $r_i = 0.6$ cm and $r_o = 1.0$ cm. The dependence of the boundary temperature Θ_o on ψ leads to a two-dimensional temperature field, i.e., $\Theta = \Theta(r, \psi)$. In this case, we have

$$(3.40) \quad c_n^{(o)} = \int_{-1}^{+1} \Theta_o(\xi) P_n(\xi) d\xi.$$

The integrals in (3.40) are evaluated numerically. Moreover, we have $c_n^{(i)} = 0$ for all n . The other coefficients are computed using the given formulae. Finally, the transformed temperature $\Theta(r, \psi)$ and consequently the physical temperature $\vartheta(r, \psi)$ are obtained.

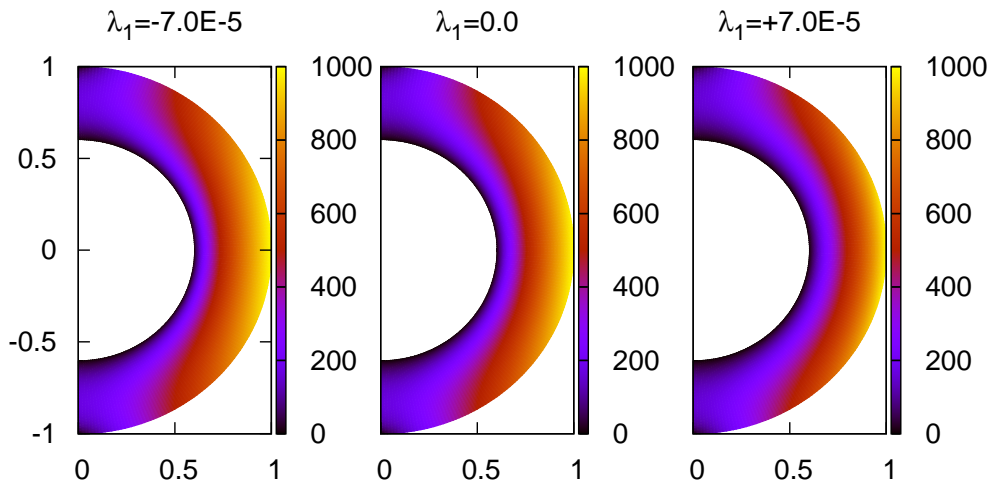


FIG. 5. Axisymmetric temperature fields in a hollow sphere with $r_i = 0.6$ cm, $r_o = 1.0$ cm, $\vartheta_i(\psi) = 0^\circ\text{C}$, $\vartheta_o(\psi) = 1000 \sin \psi^\circ\text{C}$ and $\lambda = \lambda_0 - \lambda_1 \vartheta$ with $\lambda_0 = 0.12$. Three cases are shown: constant λ , λ decreasing with temperature and λ increasing with temperature. Values of λ_1 are shown in the figure. Horizontal axis is $x = r \sin \psi$ and vertical axis is $z = r \cos \psi$. Colors map the temperature.

The temperature fields for three different cases are shown in Fig. 5. These three cases have the same material properties as of the example in Subsec. 3.2. We, again, observe that the temperature of the case with constant λ lies in between the other two cases with positive and negative λ_1 . We also observe that the high-temperature region is more extended in the case with negative λ_1 compared to other two cases.

Moreover, one-dimensional temperature profiles in the radial direction r at $\psi = \pi/2$ and in the zenithal direction ψ at $r = (r_i + r_o) / 2$ are plotted in Figs. 6

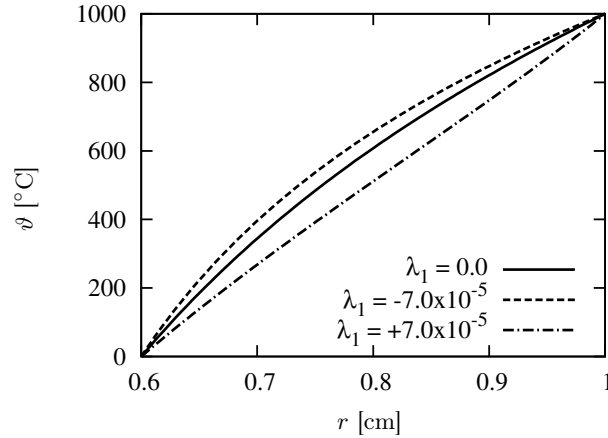


FIG. 6. Axisymmetric temperature profiles in a hollow sphere with $r_i = 0.6$ cm, $r_o = 1.0$ cm, $\vartheta_i(\psi) = 0^\circ\text{C}$, $\vartheta_o(\psi) = 1000 \sin \psi^\circ\text{C}$ and $\lambda = \lambda_0 - \lambda_1 \vartheta$ with $\lambda_0 = 0.12$. The profiles are along the radial direction r at $\psi = \pi/2$. Three cases are shown: constant λ , λ decreasing with temperature and λ increasing with temperature. Values of λ_1 are shown in the figure.

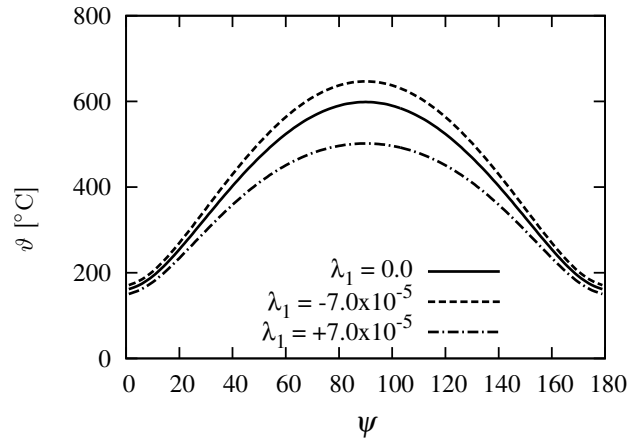


FIG. 7. Axisymmetric temperature profiles in a hollow sphere with $r_i = 0.6$ cm, $r_o = 1.0$ cm, $\vartheta_i(\psi) = 0^\circ\text{C}$, $\vartheta_o(\psi) = 1000 \sin \psi^\circ\text{C}$ and $\lambda = \lambda_0 - \lambda_1 \vartheta$ with $\lambda_0 = 0.12$. The profiles are along the zenithal direction ψ at $r = 0.8$ cm. Three cases are shown: constant λ , λ decreasing with temperature and λ increasing with temperature. Values of λ_1 are shown in the figure.

and 7, respectively. Again, we observe that the temperature is lower for the case with $\lambda_1 > 0$ and greater for the case with $\lambda_1 < 0$ as compared to the linear case with $\lambda_1 = 0$. Figure 6 shows that not only the values, but also the shape of the temperature profile is changed for different cases. However, Fig. 7 reveals that, in the zenithal direction ψ , the shape of the temperature profile is preserved and only the values are changed.

3.4. Comparison with perturbation solution

Another approach to solve the nonlinear heat equation (2.8) is the use of perturbation methods. This gives an approximate solution to the problem. Here, we compare such an approximate solution with our exact solution and examine the convergence of the perturbation series.

In order to perform a perturbation solution, we rewrite Eq. (2.8) in the following form:

$$(3.41) \quad (1 - \varepsilon\vartheta) \Delta\vartheta = \varepsilon \nabla\vartheta \cdot \nabla\vartheta.$$

Note that we have assumed a linear variation of the thermal conductivity with temperature, i.e., $\lambda = \lambda_0 - \lambda_1\vartheta = \lambda_0(1 - \varepsilon\vartheta)$ with $\varepsilon = \lambda_1/\lambda_0$. Now, we assume that the temperature field can be expressed as a power series in the small parameter ε :

$$(3.42) \quad \vartheta = \sum_{n=0}^{\infty} \varepsilon^n \vartheta_n = \vartheta_0 + \varepsilon\vartheta_1 + \varepsilon^2\vartheta_2 + \dots$$

Substituting this ansatz in Eq. (3.41), we have

$$(3.43) \quad \left(1 - \sum_{n=0}^{\infty} \varepsilon^{n+1} \vartheta_n\right) \sum_{n=0}^{\infty} \varepsilon^n \Delta\vartheta_n = \sum_{n=0}^{\infty} \varepsilon^{n+1} \nabla\vartheta_n \cdot \sum_{n=0}^{\infty} \varepsilon^n \nabla\vartheta_n.$$

Grouping terms with similar power of ε yields the following series of differential equations:

$$(3.44a) \quad \varepsilon^0: \quad \Delta\vartheta_0 = 0,$$

$$(3.44b) \quad \varepsilon^1: \quad \Delta\vartheta_1 = \nabla\vartheta_0 \cdot \nabla\vartheta_0,$$

$$(3.44c) \quad \varepsilon^2: \quad \Delta\vartheta_2 = \vartheta_0 \Delta\vartheta_1 + 2\nabla\vartheta_0 \cdot \nabla\vartheta_1,$$

$$(3.44d) \quad \varepsilon^3: \quad \Delta\vartheta_3 = \vartheta_0 \Delta\vartheta_2 + \vartheta_1 \Delta\vartheta_1 + 2\nabla\vartheta_0 \cdot \nabla\vartheta_2 + \nabla\vartheta_1 \cdot \nabla\vartheta_1,$$

which are called zeroth-, first-, second- and third-order approximations, respectively. Also, appropriate boundary conditions are to be derived. To this aim, we insert the asymptotic expansion (3.42) into Eq. (3.11). Grouping the terms with similar power of ε , we get

$$(3.45a) \quad \varepsilon^0: \quad \vartheta_0(r = r_i) = \vartheta_i, \quad \vartheta_0(r = r_o) = \vartheta_o,$$

$$(3.45b) \quad \varepsilon^1: \quad \vartheta_1(r = r_i) = 0, \quad \vartheta_1(r = r_o) = 0,$$

$$(3.45c) \quad \varepsilon^2: \quad \vartheta_2(r = r_i) = 0, \quad \vartheta_2(r = r_o) = 0,$$

$$(3.45d) \quad \varepsilon^3: \quad \vartheta_3(r = r_i) = 0, \quad \vartheta_3(r = r_o) = 0.$$

This approach can be extended to n th-order approximation. However, it demands a considerable amount of calculation effort when n is large. Here, we calculate up to the third-order approximation and compare the results of the perturbation approximations of different orders ($n \leq 3$) with the exact solution.

The results are plotted in Fig. 8 for the parameters of mild steel ($\varepsilon = 5.83 \times 10^{-4}$). We observe that although the first-order solution gives considerable improvement to the linear solution, it is not enough to get the temperature profile accurately. The second- and third-order solutions are almost

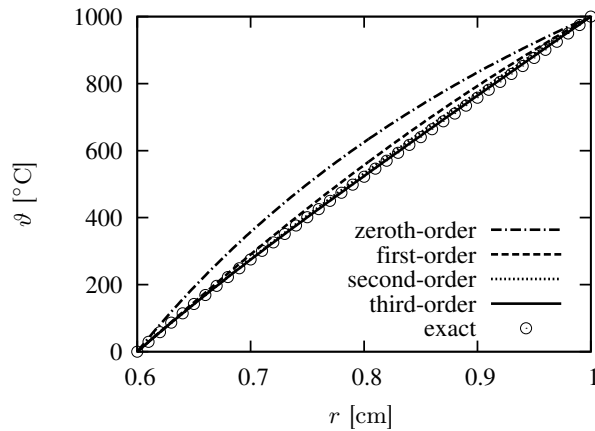


FIG. 8. Spherically symmetric temperature profiles in a hollow sphere with $r_i = 0.6$ cm, $r_o = 1.0$ cm, $\vartheta_i = 0^\circ\text{C}$, $\vartheta_o = 1000^\circ\text{C}$ and $\lambda = \lambda_0 - \lambda_1\vartheta$ with $\lambda_0 = 0.12$ and $\lambda_1 = 7 \times 10^{-5}$. Also, perturbation solutions of different orders are shown.

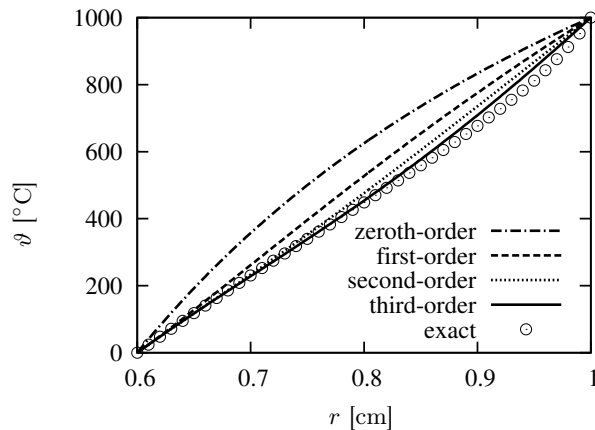


FIG. 9. Spherically symmetric temperature profiles in a hollow sphere with $r_i = 0.6$ cm, $r_o = 1.0$ cm, $\vartheta_i = 0^\circ\text{C}$, $\vartheta_o = 1000^\circ\text{C}$ and $\lambda = \lambda_0 - \lambda_1\vartheta$ with $\lambda_0 = 0.12$ and $\lambda_1 = 1 \times 10^{-4}$. Also, perturbation solutions of different orders are shown.

indistinguishable from the exact solution. The first-order perturbation solution is often used in approximations of nonlinear equations. Here, we see that only a first-order approximation does not produce accurate results. If we increase the perturbation parameter, say $\varepsilon = 8.33 \times 10^{-4}$, then even the second- and third-order solutions deviate from the exact one, as shown in Fig. 9.

4. Conclusions

In this paper, we have developed an exact analytical solution for steady nonlinear heat conduction equation with temperature-dependent thermal conductivity in hollow spherical objects. For this purpose, we have employed an integral transform which transforms the nonlinear equation into a linear one (the Laplace equation). Once the Laplace equation is solved for the transformed temperature subjected to transformed boundary conditions, one can compute the physical temperature using the inverse transform. Two problems are solved for demonstration of the proposed solution. First, the temperature field in a hollow sphere with spherical symmetry is investigated. This is a one-dimensional problem in the radial direction. Second, we solve for the axisymmetric temperature field in a hollow sphere which is a two-dimensional problem. Finally, we investigated perturbation solutions of the one-dimensional problem and compared them with the exact solution. With this, we are able to examine the convergence of the perturbation solutions.

References

1. R. TROSTEL, *Instationäre Wärmespannungen in einer Hohlkugel*, Ingenieur-Archiv, **24**, 373–391, 1956.
2. R. SHIRMOHAMMADI, A. MOOSAIE, *Non-Fourier heat conduction in a hollow sphere with periodic surface heat flux*, Int. Commun. Heat Mass Transf., **36**, 827–833, 2009.
3. A. MOOSAIE, *Axisymmetric non-Fourier temperature field in a hollow sphere*, Arch. Appl. Mech., **79**, 679–694, 2009.
4. R. TROSTEL, *Stationäre Wärmespannungen mit temperaturabhängigen Stoffwerten*, Ingenieur-Archiv, **26**, 416–434, 1958.
5. R. TROSTEL, *Wärmespannungen in Hohlzylindern mit temperaturabhängigen Stoffwerten*, Ingenieur-Archiv, **26**, 134–142, 1958.
6. A. AZIZ, T.Y. NA, *Periodic heat transfer in fins with variable thermal parameters*, Int. J. Heat Mass Transf., **24**, 1397–1404, 1981.
7. F. KHANI, A. AZIZ, *Thermal analysis of a longitudinal trapezoidal fin with temperature-dependent thermal conductivity and heat transfer coefficient*, Commun. Nonlinear Sci. Numer. Simul., **15**, 590–601, 2010.

8. O.D. MAKINDE, R.J. MOITSHEKI, *On solutions of nonlinear heat diffusion model for thermal energy storage problem*, Int. J. Physical Sciences, **5**, 246–250, 2010.
9. *VDI-Gesellschaft Verfahrenstechnik und Chemieingenieurwesen*, Wärmeatlas, Springer, Berlin 2006.

Received March 11, 2012; revised version May 29, 2012.
